Ionic Dimethacrylates for Antimicrobial and Remineralizing Dental Composites

Bienek DR[1]*, Frukhtbeyn SA[1], Giuseppetti AA[1], Okeke UC[1], Pires RM[2], Antonucci JM[3] and Skrtic D[1]
[1]Volpe Research Center, ADA Foundation, Maryland, USA
[2]Chemical and Biological Sciences, Montgomery College, Maryland, USA
[3]Biomaterials Group, Biosystems and Biomaterials Division, National Institute of Standards and Technology, Maryland, USA

Abstract

Two ionic dimethacrylates (IDMA1 and IDMA2) intended for utilization in multifunctional, antibacterial and remineralizing dental resins and composites were synthesized by nucleophilic substitution reactions. Crude IDMAs were purified by multi-step extraction from ethanol-diethyl ether-hexane solvent system. Their structures were validated by nuclear magnetic resonance and mass spectrometry. As evidenced by the water contact angle measurements ((63.2-65.5)º), IDMAs did not affect the wettability of urethane dimethacrylate (UDMA)-based copolymers (average contact angle ((60.8±5.1)º). The attained degrees of vinyl conversion increased from 88.1% (no-IDMA control) up to 93.0% (IDMA2 series). Flexural strength (FS) of copolymers was reduced from 94.8 MPa (control) to (68.9-71.8) MPa (IDMA counterparts) independent of monomer type and/or its concentration. This reduction in FS should not disqualify IDMAs from consideration as viable antibacterial agents in multifunctional restoratives. Tested at concentrations exceeding the expected leachability of unreacted monomers from cured copolymers and/or composites, IDMAs had no deleterious effect on viability and/or metabolic activity of fibroblasts. The remineralization potential of amorphous calcium phosphate IDMA/UDMA composites was confirmed by calcium and phosphate ion release kinetic experiments. Results of this study warrant in-depth biological, physicochemical, mechanical and antibacterial assessments of IDMA resins and composites to identify prototype(s) suitable for clinical testing.

Keywords: Dental, Composite, Antimicrobial, Remineralizing, Amorphous calcium phosphate; Antibacterial monomers; Biocompatibility

Introduction

Present-day dental resins and composites are aesthetically pleasing while recuperating tooth's anatomy and function [1,2]. However, typically unstable restoration/tooth interface [3,4] often results in gap formation, increased bacterial microleakage, and ultimately, secondary caries. Bioactive restoratives release remineralizing ions [5-8] and provide protection against tooth demineralization by regenerating mineral lost to decay. One of the remineralizing approaches utilizes amorphous calcium phosphate (ACP) [8-13]. Our group's research on ACP-based restoratives has yielded polymeric materials with sustained remineralizing action. This approach, however, provides no protection against microbes at the site of restoration. The lack of substantial antimicrobial (AM) properties [1,2], verifiable in clinical trials [14], makes ACP restoratives susceptible to recurrent dental caries.

Historically, developments of AM dental restoratives were focused mainly on resin modification, simply because it appeared easier to alter the resinous phase than fillers. Additives like chlorhexidine were first used over 30 years ago [15]. Chlorhexidine, antibiotics, zinc, silver (Ag) nanoparticles, fluoride, and iodide [16-19] release rapidly and provide short-term AM protection. Release kinetics of the AM agent is typically accompanied with diminished performance due to increased porosity [4,15] and toxicity to surrounding tissues [16,17,19]. These insufficiencies put emphasis on development of new AM agents [20].

Emergence of new AM monomers has been discussed in a recent review [21]. Amongst frequently studied quaternary ammonium (QA) AM agents, greatest attention has been given to methacryloyloxydo decyl pyrimidinium bromide (MDBP) [1,2, 22-24]. Due to MDBP color instability, its use is frequently restricted to repairs where aesthetics is of no concern. In 2012, ionic dimethacrylates (IDMAs) were patented [25] and proposed for utilization in dental applications. The observed AM effect of IDMA generally resembled the effect of MDBP incorporated into 2,2-bis[p-(2-hydroxy-3-methacryloxypropoxy) phenyl] propane (Bis-GMA)/triethylene glycol dimethacrylate (TEGDMA) matrices [26]. Subsequently, AM properties of QA dimethacrylates in bacterial biofilms were assessed [27-30].

The initial studies only tangentially addressed IDMA's biocompatibility with human cells [31]. Cytotoxicity experiments utilizing mouse macrophage-like cells revealed no toxicity at 10% IDMA levels and reduced viability and metabolic activity at higher concentrations. Li *et al.* [29] used human gingival fibroblasts to assess cytotoxicity of eluents from primer/adhesive containing QA dimethacrylates and found no toxicity compared to the no-AM control. In these studies, leached extracts were not quantified and the IDMA concentration in eluent samples remained unknown. Further, AM agents' purity was not reported and the accompanying structural characterizations appear incomplete.

Our objectives were to synthesize 2-(methacryloyloxy)-N-(2-(methacryloyloxy)ethyl)-N,N-dimethylethan-1-aminium bromide (IDMA1) and N,N'-([1,1'-biphenyl]-2,2'-diylbis(methylene)) bis(2-(methacryloyloxy)-N,N-dimethylethan-1-aminium) bromide (IDMA2); assess purity, validate the structures; incorporate IDMAs into light-cured urethane dimethacrylate (UDMA), polyethylene glycol-extended UDMA (PEG-U)/ethyl 2-(hydroxymethyl) acrylate (EHMA) resin (designated UPE resin); and assess IDMA/UPE resin hydrophobic/hydrophilic balance, degree of vinyl conversion (DVC), flexural strength (FS), and elastic modulus (E). As potential leaching of unreacted monomers and other products can lead to clinical failure [32], we assessed *in vitro* cytotoxicity of the IDMAs. Also, we synthesized and validated ACP filler, incorporated ACP into UDMA-based resins, and assessed the remineralizing potential of the ensuing composite.

Materials and Methods

IDMA syntheses

IDMA1 and IDMA2 syntheses are schematized in Figure 1. For IDMA1 synthesis, 10 mmol 2-(N,N-dimethylamino) ethyl methacrylate

*Corresponding author: Diane Bienek, ADA Foundation, Volpe Research Center, Gaithersburg, USA

(DMAEMA; Sigma-Aldrich Co., USA), 10 mmol 2-bromoethyl methacrylate (BEMA; Sigma-Aldrich Co.), 1 mmol butylated hydroxytoluene (BHT; Sigma-Aldrich Co.), and 2.5 mL of chloroform (CHCl$_3$; Sigma-Aldrich Co.) were mixed in a reaction vessel equipped with a reflux column. The reaction mixture was heated (50-55 ºC for 24 h) and washed with hexane (Sigma-Aldrich Co.). The crude IDMA1 was purified by extraction with an ethanol-diethyl ether-hexane solvent system. IDMA2 was synthesized by reacting DMAEMA (10 mmol) and 5 mmol 2,2'-bis (bromomethyl)-1,1'-biphenyl (bBrMbP; Sigma-Aldrich Co.) under conditions/experimental steps identical to those in the IDMA1 synthesis. Purified products were freeze-dried overnight and remaining impurities were removed using CHCl$_3$.

IDMAs structural/compositional analysis

IDMAs ^{1}H NMR spectra were obtained using a Bruker Avance 2 (600 MHz) spectrometer (Bruker Corp., USA) equipped with a broadband observe room temperature probe. Samples were run using deuterated chloroform (CDCl$_3$; Sigma-Aldrich Co.) (IDMA1) or deuterated dimethyl sulfoxide (DMSO-d6; Sigma-Aldrich Co.) (IDMA2) as solvents, and tetramethylsilane (TMS) as an internal standard. Concentrations of the samples analyzed varied, but were generally within 0.1-0.5 M. Heteronuclear single quantum coherence (HSQC) experiments were employed for spectra signal assignation.

Mass spectrometer (QuattroMicro, Waters Corp., USA) was operated in the positive ionization mode. Three kV potential was applied to the electrospray ionization needle and the de-solvation temperature was set at 250 ºC. Nitrogen flow and sample injection rates were 500 L/h and 10 µL/min, respectively.

Biocompatibility tests

Immortalized NCTC clone 929 [L-cell, L-929, Strain L derivative] (ATCC®CCL-1™) mouse subcutaneous connective tissue fibroblasts were obtained from American Type Culture Collection (ATCC, USA). This cell line was selected for cytotoxicity testing as it is deemed by the American Society for Testing and Materials to be readily available,

well-established, and yielding reproducible results [33,34]. Cells were maintained (37 ˚C, 5% CO$_2$) in Eagle's minimum essential medium (ATCC) supplemented with 10% horse serum (ATCC). For experiments, cells were obtained from a subconfluent stock culture. Cell viability was determined on an improved Neubauer hemocytometer using trypan blue staining and bright field microscopy. Falcon™ 96-well flat-bottom tissue culture-treated microplate (black with clear bottom) was seeded with 20,000 viable cells/well. After 48 h incubation, cells were exposed to two-fold serial dilutions of IDMA1 or IDMA2. These dilutions (≤ 10.66 mmol/L IDMA1 and ≤ 5.7 mmol/L IDMA2) were selected to approximate the maximum possible exposure, assuming 7% mass fraction of IDMA in the composite with a maximum of 2% leaching. These guidelines are based on results of an accelerated ACP UDMA/PEG-U/2-hydroxyethyl methacrylate (HEMA) leachability study [35]. Negative controls consisted of wells without the IDMAs and/or cells. After 24 h and 72 h IDMA exposure, cultures were assessed for viability and metabolic activity. Each IDMA was tested in triplicate on five independent occasions.

Cell viability was assessed using the LIVE/DEAD® Viability/Cytotoxicity Kit (Life Technologies, Corp., USA). After IDMA exposure, cells were washed with Dulbecco's phosphate-buffered saline (without calcium (Ca) and magnesium) and subsequently incubated with ethidium homodimer-1 (1 µM) and 0.658 µM calcein acetoxymethyl ester (hereafter calcein) for 20 min at room temperature. These optimal stain concentrations were determined by serial dilution analyses. Spectra Max M5 plate reader (Molecular Devices, Corp., USA) was used to assess fluorescence of ethidium homodimer-1 (excitation 530 nm, emission 645 nm) and calcein (excitation 485 nm, emission 530 nm). Assay controls included live and dead (70% methanol-treated; 30 min) cells that were exposed to calcein and/or ethidium homodimer-1. As per the manufacturer, these values were used to estimate the live and dead cells percentage. As previously reported [36], inter-assay control limits were set for these wells (value of each triplicate well needed to be within 20% of their mean).
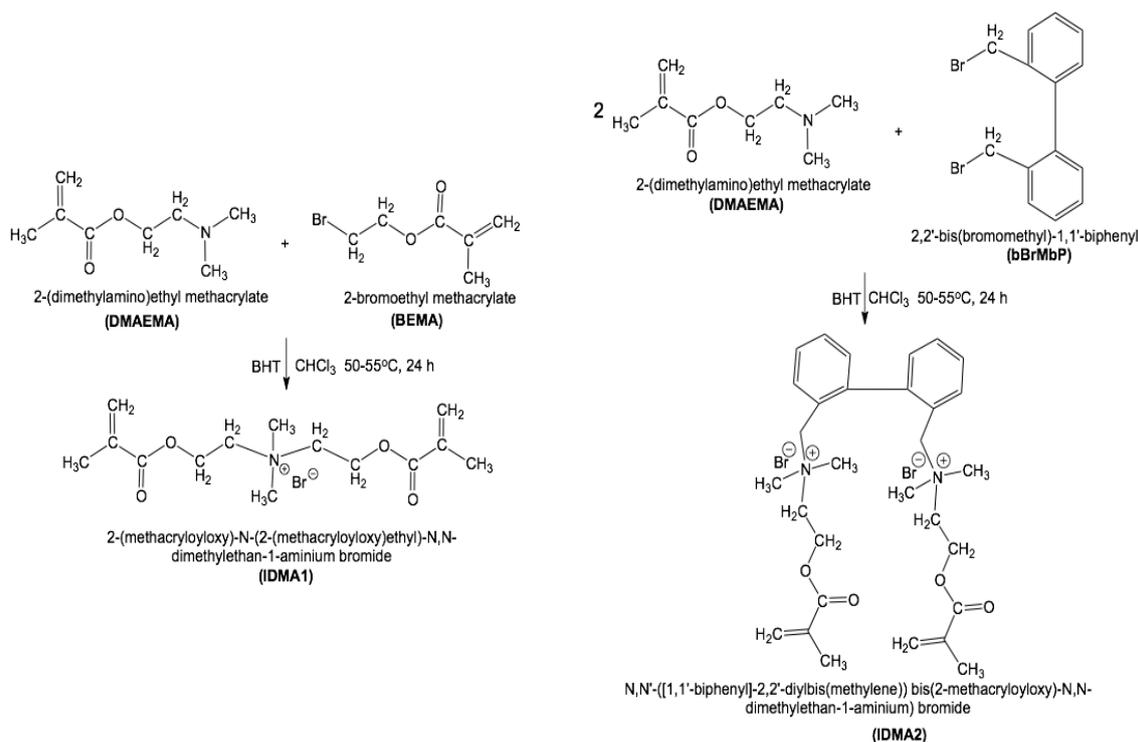

Figure 1: Schematic presentation of IDMA1 (left) and IDMA2 (right) synthesis.

Citation: Bienek DR, Frukhtbeyn SA, Giuseppetti AA, Okeke UC, Pires RM, et al. Ionic Dimethacrylates for Antimicrobial and Remineralizing Dental Composites. Ann Dentist Oral Disord 2018; 1:108.

After completing the viability assay, the supernatant was removed and each well received 200 µL culture medium and 40 µL CellTiter 96® AQueous One Solution Reagent (Promega, USA). Plates were then incubated for 40 min at 37 ˚C in a 5% CO_2 environment. Optical densities were determined using an Epoch microplate spectrophotometer (BioTek Instruments, Inc., USA) set at 490 nm. To normalize assay responses, the optical densities were transformed into the percent increase or decrease of that observed in the control group (no monomer). Assay controls included wells that only contained an equal volume of culture medium.

Resin evaluation

UPH/UPE resin was formulated by blending 50.91% w/w UDMA (Esstech, USA), 18.18% w/w PEG-UDMA (Esstech, Essington) and 30.91% w/w HEMA (Esstech, Essington) or EHMA (Sigma-Aldrich Co). 0.2% w/w camphorquinone (CQ; Sigma-Aldrich Co) and 0.8% w/w ethyl-4-N,N-dimethylamino benzoate (4EDMAB; Sigma-Aldrich Co.) were utilized as the polymerization initiators. IDMAs were added into UDMA-based UPE resin at 10 or 20 mass %. Formulated resins were pipetted into stainless steel molds (for contact angle evaluation, 13 mm diameter, 1.4 mm height) or hollow glass beams (for DVC, FS, and E measurements, 1.9×1.9×25 mm), open sides of the molds/beams were covered (Mylar film/glass slide for metal molds, Parafilm/wax for glass beams). Each sample was irradiated for 120 s from two sides (Triad 2000, Dentsply International, USA). After curing, samples were de-molded and kept in the dark, under vacuum, for ≥ 24 h before testing. The rationale for the chosen IDMA concentrations was that 10 mass % IDMA in Bis-GMA/TEGDMA polymers significantly reduced bacterial attachment, while 30 mass % IDMA did not further reduce bacterial coverage while diminishing macrophage density and activity [31].

Changes in water contact angle (sessile drop technique) were used to express variations in UPE resin hydrophobicity/hydrophilicity upon introduction of IDMAs. A drop shape analyzer DSA-100 (Krüss USA, USA) was employed for the measurements (four replicates per experimental group) performed according to the manufacturer's instructions.

Near-IR spectroscopic method that monitors the reduction in =C-H absorption band at 6165 cm^{-1} in the overtone region was used to determine the DVC of (IDMA1 or IDMA2)/UPE copolymers. By maintaining constant specimen thickness, the need to use an invariant absorption band as an internal standard was circumvented. Near infrared spectra were collected before photo-cure and 24 h post-cure. There were three replicate measurements per experimental group.

The three-point bending tests were conducted on a Universal Testing Machine (MTS Systems Corp., USA). Polymerized UPE and UPE-IDMA beams (1.9×1.9×25 mm) were centered between two supports (20 mm apart) and a bending load was applied to the center point at a velocity of 1 mm/min. Flexural strength (maximum load) and elastic modulus (ratio of elastic stress to strain; E) were determined for each sample. There were three replicate measurements per experimental group.

Remineralizing ACP composites

ACP was synthesized utilizing well-established protocols [8,35,37]. Amorphousness of the filler was validated by Fourier transform infrared spectroscopy (FTIR; Nicolet Magna-IR FTIR 550, ThermoFisher Scientific, USA) and X-ray diffraction (XRD; Rigaku X-ray diffractometer, Rigaku/USA Inc., USA). Particle size distribution (PSD; SA-CP3 analyzer, Shimadzu Scientific Instruments Inc., USA) was assessed before (as-made ACP) and after milling (5 g of ACP in 15 g of 1-propanol (Sigma-Aldrich Co.); 2 h at 200 rpm, Pulverisette 7 ball mill (Fritsch, Germany).

ACP was dispersed in 1-propanol, sonicated 1 h in a water bath, and mixed with the appropriate amount of UPH resin to yield composite of homogeneous appearance containing 60 mass % resin and 40 mass % ACP filler. Solvent was evaporated at 22℃, under vacuum (overnight) and continuous magnetic stirring. The composite paste was tightly packed into stainless steel molds (13 mm diameter, 1.4 mm height). Both sides of the mold were covered sequentially with Mylar film and a glass slide. The assembly was clamped and each side irradiated for 120 s with visible light (Triad 2000, Dentsply International, York, PA). After curing, samples were de-molded and kept in the dark, under vacuum, for ≥ 24 h before testing.

Composite disk specimens were individually immersed in 90 mL of 4-(2-hydroxyethyl) piperazine-1-ethanesulfonic acid (HEPES; Sigma-Aldrich Co.)-buffered (pH 7.4) 0.13 M NaCl (Sigma-Aldrich Co.) solution. Solutions were replaced with fresh buffers at 1, 2, 4, 8, and 16 weeks. Solution Ca and phosphorus (P) concentrations were determined by atomic emission spectroscopy (Prodigy High Dispersion ICP, Teledyne Leeman Labs, USA).

Statistical analyses

The number of specimens for each evaluation step was chosen so that there was a reasonable chance (power) to detect the minimum desired difference between groups [38]. Variance estimates were based on previous work or literature. Analysis of variance (ANOVA), graphical data analysis and other related tests [39] were used to analyze experimental data as a function of material makeup, storage/exposure time, or any other relevant factor included in the experimental design. When overall statistically significant effects were found with ANOVA, multiple comparisons (2-sided, α=0.05) were used to determine significant differences between groups (SigmaPlot™ 11.0; Systat® Software, Inc., USA or Excel 2016, Microsoft Corp., USA. Assumptions of normality were evaluated using the Shapiro Wilks analysis of variance test for normality [40] for experiments with ≥ 5 replicates. Graphics were created using Excel 2016 or DeltaGraph6 for Windows® (Red Rock Software, Inc., USA).

Results

IDMAs: Structural validation

^{1}H NMR confirmed the assigned structure of the IDMAs. Signals from the IDMA ^{1}H NMR ($CDCl_3$, ppm relative to tetramethylsilane) spectrum were assigned to: 6.15 (2H, s); 5.67 (2H, s); 4.71 (4H, m); 4.31 (4H, m); 3.63 (6H, s); and 1.95 (6H, s), as reported [36]. Signals from the IDMA2 ^{1}H NMR spectrum were assigned to: 7.82 (2H, m); 7.69 (2H, t); 7.63 (2H, t); 7.52 (2H, m); 6.03 (2H, s); 5.75 (2H, s); 4.63 (2H, d); 4.22 (4H, b); 4.04 (2H, d); 3.59 (2H, m); 3.30 (2H, m); 2.93 (6H, s); 2.66 (6H, s); and 1.87 (6H, s)[36].

Mass spectroscopy

IDMA1 yielded two pronounced peaks at m/z 270.35 ($C_{14}H_{24}NO_4^+$, calculated m/z 270.17) and 113.06 ($C_6H_9O_2^-$, calculated m/z 113.06), as shown in Figure 2(a). IDMA2 yielded prominent peaks at m/z 573.55/575.58, ($C_{30}H_{42}N_2O_4^{2+}Br^-$, calculated m/z 573.23/575.23); 416.33/418.29 ($C_{22}H_{27}NO_2^+Br^-$, calculated m/z 416.12/418.12); 179.18 ($C_{22}H_{34}N_2O_2^{2+}$, calculated m/z 179.13); 113.07 ($C_6H_9O_2^-$, calculated m/z 113.07) (Figure 2(b)).

IDMAs biocompatibility

The overall effect of IDMA1 concentration (2-factor ANOVA; $P \le 0.05$) at 24 h or 72 h exposure time was found to be significant for only the highest IDMA concentration by multi-pair comparison tests (50% and 60% lower at 24 h and 72 h, respectively) (Figure 3). Like the effect of IDMA concentration, time of IDMA1 exposure was also found significant (2-factor ANOVA; $P \le 0.05$). While being apparently lower at any given concentration after 72 h exposure, the observed reduction was significantly different (2-factor ANOVA; $P \le 0.05$) at
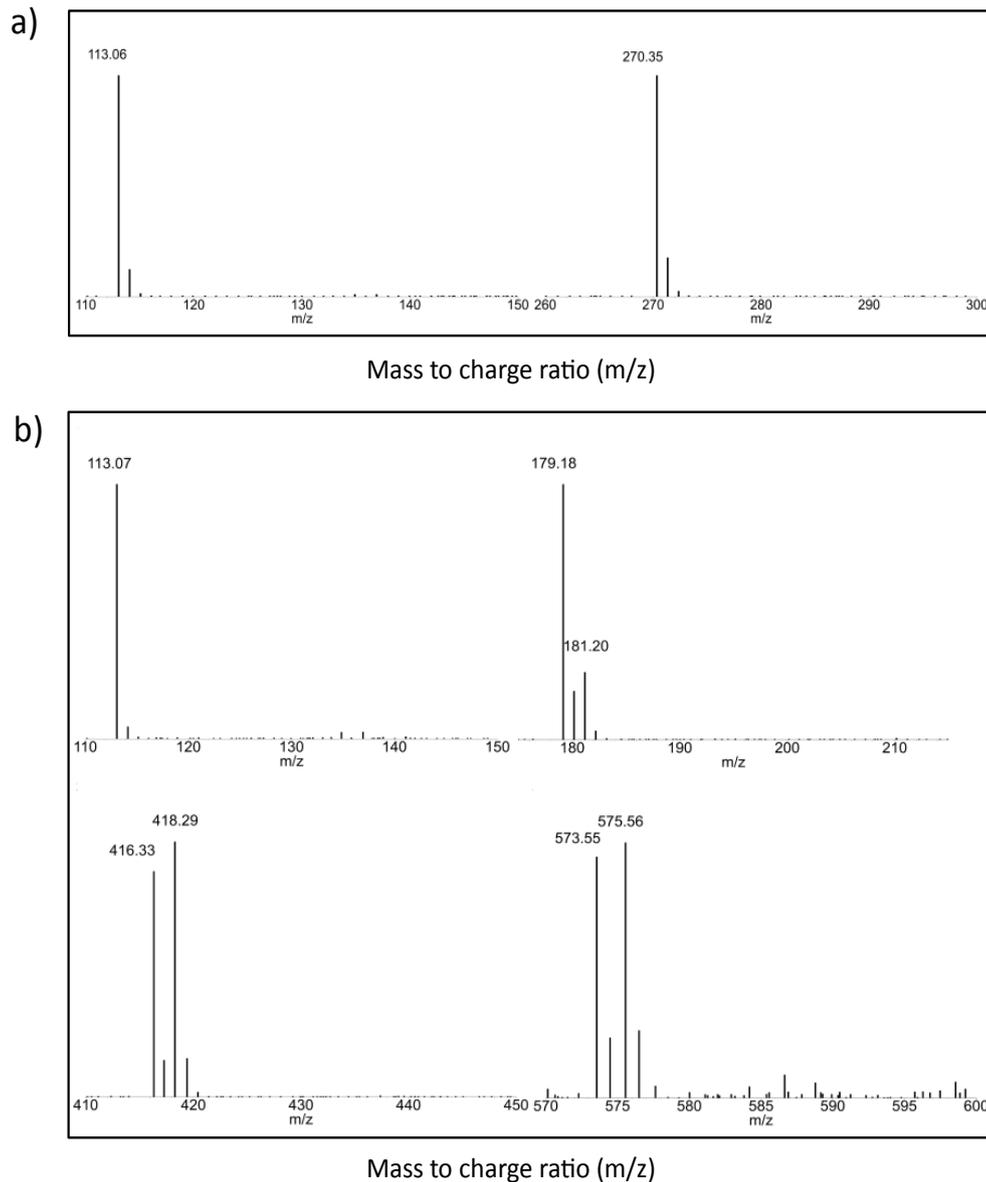
Figure 2: Mass spectra of IDMA1 (a) and IDMA2 (b).

high (10.66, 5.33, and 2.67 mmol/L) and 0.08 µmol/L IDMA1 levels. In contrast to IDMA1, IDMA2 did not significantly affect metabolic activity. The modest reduction (~4%) generally seen at 72 h compared to 24 h exposure was not statistically different. Control wells containing no cells yielded a negligible optical density value, which did not differ statistically between treatment days. Similarly, control wells (with or without cells) in which CellTiter 96® AQueous One Solution Reagent was omitted, yielded low optical density values. Positive control wells, containing unexposed cells that were given an equal volume of culture medium, were not statistically different from cells that were previously stained with live-dead stain (data not shown).

Like metabolic activity, cell viability data also showed the significant effect of IDMA1 concentration (2-factor ANOVA; $P \leq 0.001$). Pairwise comparisons indicated that for 24 h exposure, IDMA1 did not adversely affect the number of live cells. However, after 72 h of exposure to 10.66 mmol/L IDMA1, cellular viability was reduced at least 50% (2-factor ANOVA; $P \leq 0.05$) (data not shown).

Viability and metabolic activity of cells exposed to IDMA1 for 24 h showed a positive linear correlation for concentrations ≤ 5.33 mmol/L (Figure 4). At 10.66 mmol/L IDMA1, a similar number of viable cells had decreased metabolic activity. After 72 h exposure, correlation between live cells and their metabolic activity was characterized by $R^2=0.86$ (coefficient of determination; $P \leq 0.02$). In contrast to IDMA1, the highest concentration of IDMA2 did not exert a deleterious effect on fibroblasts viability. Viability and metabolic activity of cells exposed to IDMA2 for 24 h showed a correlation ($R^2=0.626$; $P \leq 0.02$). However, at 72 h, the correlation between metabolic activity and viability was insignificant.

Effect on physicochemical properties of UDMA-based resin

Wettability of IDMA-containing UPE resins was unaffected by either the type or the concentration of IDMA incorporated into the UPE matrix (Table 1). Introduction of IDMAs, generally, increased the DVC: the effect ranged from marginal (1.8% increase for IDMA1 at 20
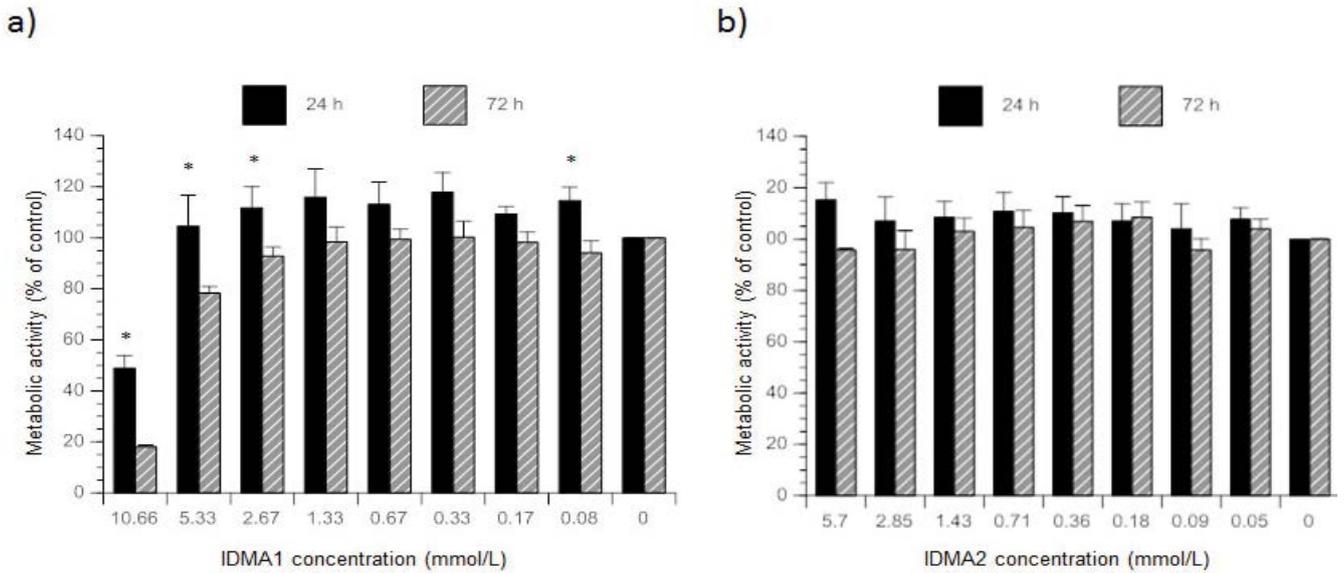
Figure 3: Metabolic activity of fibroblasts exposed to various IDMA1 (a) or IDMA2 (b) concentrations. Indicated are mean value ± SEM for five or more independent replicates tested in triplicate. * indicates $P \le 0.05$ when comparing exposure time within a monomer concentration.
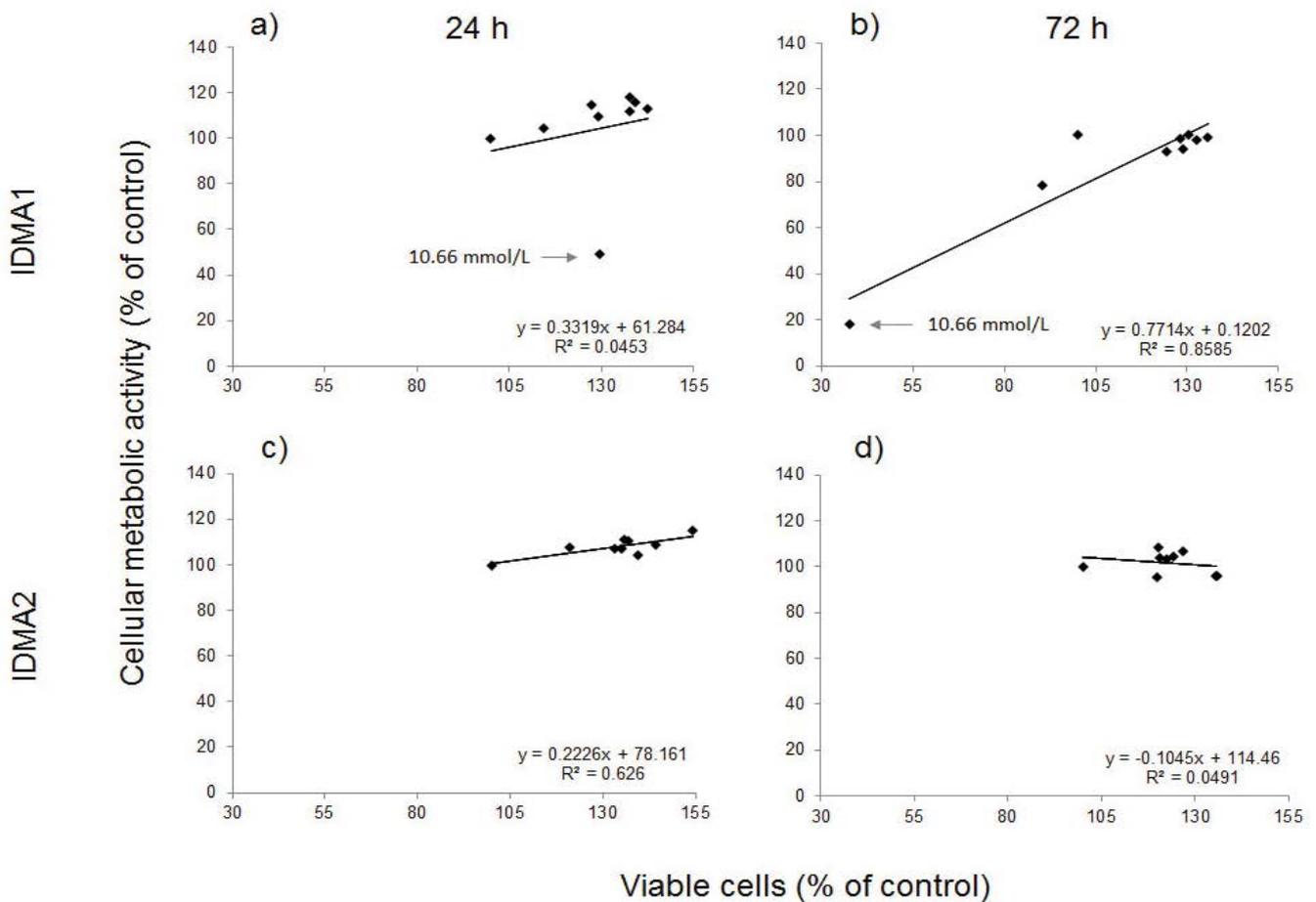

Figure 4: Correlation between the cellular metabolism and viability of fibroblasts exposed to IDMA1 (a and b) or IDMA2 (c and d) for 24 or 72 h, respectively. Data represent five or more independent replicates. → indicates cellular response observed with 10.66 mmol/L IDMA1.

Resin	Contact angle (°)	DVC (%)	FS (MPa)	E (GPa)
UPE (control)	60.8± 5.1[a]	88.12± 0.88	94.8± 5.0	2.29± 0.10
UPE-IDMA1 (10 mass %)	64.8± 4.8	92.13± 0.46	71.8± 3.4	1.79± 0.08
UPE-IDMA1 (20 mass %)	63.2 ± 3.4	89.68 ± 0.70	70.3 ± 3.0	1.70 ± 0.07
UPE-IDMA2 (10 mass %)	64.2± 3.4	92.95± 0.70	70.9 ± 3.9	1.78± 0.18
UPE-IDMA2 (20 mass %)	65.5 ± 3.2	92.49 ± 1.00	68.9 ± 2.6	1.70 ± 0.09

[a]represents mean values ± SD obtained from four independent replicates per group

Table 1: Wettability, degree of vinyl conversion (DVC), flexural strength (FS), and modulus of elasticity (E) of the experimental IDMA/UPE resins and non-IDMA control.

mass % level) to significant (4.6%-5.5%) for all other IDMA systems. Both FS and E of copolymers were reduced on average 25% by IDMA addition. The effect was independent of AM monomer type and its concentration.

ACP filler and remineralizing ability of ACP composites

XRD spectra of ACP showed patterns typical for non-crystalline substances (Figure 5). Corresponding FTIR spectra exhibited PO_4 stretching and PO_4 bending wide bands in the region of 1200-900 cm^{-1} and 630-500 cm^{-1}, respectively. PSD measurements revealed a 45% reduction of the particle median diameter (d_m) due to milling (4.93±0.52) μm to (2.73±0.17) μm in going from as-made to milled ACP. The overall PSD range remained unaltered by milling; particle sizes ranged from submicron to 70 μm.

Ion release data indicated that a desired ACP's remineralization potential was maintained in the immersing solutions of as-made and milled ACP composites. Average solution Ca/P ratios for as-made (1.59±0.03) and milled (1.66±0.03) ACP were close or identical to the Ca/P value of the stoichiometric hydroxyapatite (1.66). This immersing solution was highly conducive to tooth mineral re-deposition. It is important that subtle differences in ion release profiles between the as-made and milled ACP formulations became practically insignificant once the atomic emission spectroscopy data are normalized to disk specimen volume (Figure 6).

Discussion

AM filler studies involving different Ag forms [17,41-44], pulverized polymers [45], and/or QA polymeric nanoparticles [46] generally lack the mechanistic understanding of the AM action. Poor color stability [42-44], toxicity, questionable long-term efficiency, non-homogeneous PSD, particle leachability, and general wear undermine the materials effectiveness. These disadvantages question the feasibility of filler modification as a practical way to design AM dental restoratives.

Preferred alternatives to AM fillers entail use of various QAs in resins and nanocomposites [28,47-53]. Since 2012, Dr. Xu's group has combined QA dimethacrylates and nanosized Ag filler in Bis-GMA/ TEGDMA matrix [27] and demonstrated a synergistic AM action against bacterial biofilms with AM effects extending throughout the 12-month water-aging [28]. The AM synergy of these AM agents was reported in additional studies [29,30]. However, the explanation of how QA dimethacrylates and nanosized Ag, achieve this synergistic effect remained unanswered. Also, AM QAs incorporation dental resin composites above a certain limit significantly diminishes the materials mechanical strength [20]. Further, salivary proteins can dramatically decrease the AM activity due to the electrostatic interactions with QA functionalities [20,42]. Toxicity studies [54-56] have indicated that QAs destruct cell membrane integrity, and eventually lead to the complete breakdown and necrotic cell death.

The lack of mechanistic understanding QA-AM action warrants comprehensive evaluation of all restorative materials that incorporate these AM agents.

In this study, IDMAs structural analyses and purification were undertaken as a first step of an all-encompassing design. IDMA1 has previously [31] been characterized with misciblity with conventional resins and the unaltered processability of corresponding composites. At 10 mass % levels, purified IDMAs were easily incorporated into UDMA-based experimental resin and the ensuing AM and remineralizing (AMRE) composites. At 20% level, IDMA1 precipitated out and IDMA2 increased the overall resin viscosity to the extent of making it unprocessable. These findings do not jeopardize the intended use of IDMAs in AM copolymers and/or AMRE composites at 10 mass % level.
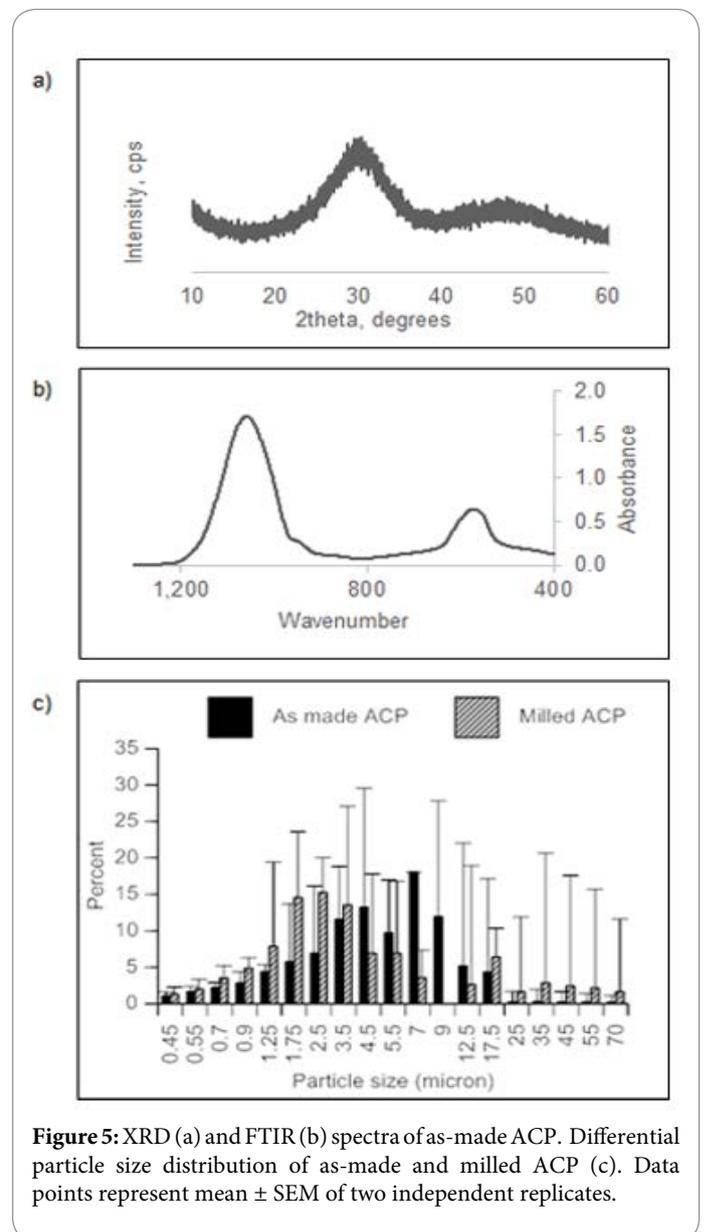

Figure 5: XRD (a) and FTIR (b) spectra of as-made ACP. Differential particle size distribution of as-made and milled ACP (c). Data points represent mean ± SEM of two independent replicates.

Although AM properties of QA dimethacrylates are frequently reported for dental applications, there is a paucity of biocompatibility data. Prior cytotoxicity experiments involved mouse macrophage-like cells (RAW 264.7) [31]. Briefly, after contact for 24 h, polymers with 10% IDMA1 significantly reduced cell density, while not affecting viability or metabolic activity. At 20% and 30% IDMA1, cell viability and metabolic activity were reduced. By evaluating residual cells that remained (after polymer disk removal), they reported that leachables did not significantly affect microphage-like cells. Using human gingival fibroblasts, Li *et al.* [29] concluded that eluents from cured primer/adhesive containing QA dimethacrylates exhibit toxicity comparable to controls. In the abovementioned studies, the leachables were not quantified. Consequently, the IDMA1 concentration in the sample and its cytotoxic potential remained undetermined. Our experiments, using known IDMA concentrations indicated that in direct contact with fibroblasts, these monomers do not adversely affect cell viability and/or metabolic activity. While at the highest concentration, IDMA1 reduced metabolic activity of the cells, we deem both IDMAs as suitable AM candidates, as our experiments approximated the maximum possible exposure, which would be released over the service life of the restorative material (i.e., years).

We foresee the results of the *in vitro* toxicity testing of any potential AM agent as a major determinant on whether a new material should undergo further evaluation. The toxicity study should be performed under conditions that reflect the expected unreacted monomer leaching. In our system, as consequence of high DVCs attained, leachables should not exceed levels typically seen in commercial materials. Therefore, IDMAs biocompatibility was assessed at concentrations representing accelerated leaching as detected in UDMA-based resins [35]. Our results confirmed the hypothesis that IDMAs exerted minimal or no toxicity towards mammalian cells. Nonetheless, future evaluations of the genotoxic, immunotoxic, and inflammatory potential would be judicious.

Lessons learned from drug discovery systems indicate that the limitations of 2-D cultures do not have a histiotypic architecture. Cells in the *in vivo* environment interact with other cells and extracellular matrix in a 3-D architecture. Consequently, 2-D cultures can provide misleading and non-predictive data for *in vivo* responses (reviewed by [57]). Cultured monolayers have also been reported to have deficiencies in cytokine release (reviewed by [58]) and cell differentiation (reviewed by [59]). Thus, our future cytotoxicity evaluations will include use of a more clinically relevant, 3-D co-culture that allows the evaluation of materials in a flow-through microfluidic system [60].
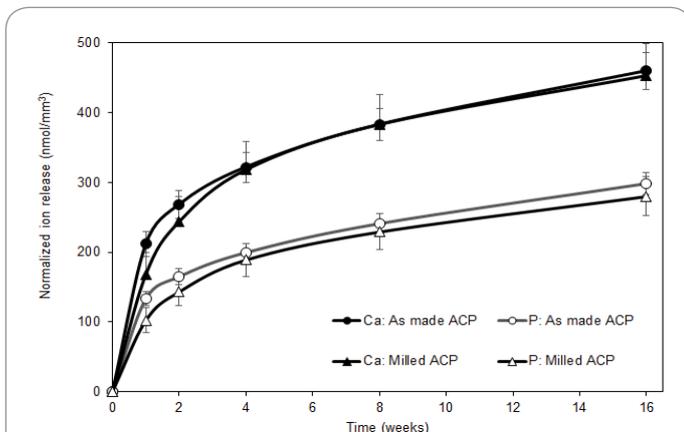

Figure 6: Ion release profiles (atomic emission spectroscopy data; shown are mean value ± SD for 5 replicate runs) for ACP (as-made or milled; as indicated) UDMA/PEG-U/HEMA composites. Data normalized with respect to the individual composite specimen's volume.

Our past research [37,61,62] indicates that the improved physicochemical and remineralizing performance of resins and their ACP composites is attainable by incorporating a more flexible base monomer UDMA instead of Bis-GMA in the resin. Combining UDMA with PEG-U, and adding HEMA or EHMA instead of TEGDMA, in UDMA-based resins, further improved the resins DVC [61,62] without increasing the polymerization stress generated in these matrices. Moreover, in UDMA/PEG-U/(HEMA or EHMA) systems, high polymerization shrinkage which typically accompanies high DVCs could be buffered by material's hygroscopic expansion. Our experimental UDMA/PEG-U/(HEMA or EHMA)/IDMA resins attained DVCs (89.7%-93.0%) that significantly exceed DVC values previously reported for Bis-GMA/TEGDMA/IDMA formulations (67.9%-70.7%)[31]. These DVCs are high enough to ensure that polymer chain mobility is minimized and, consequently, the leachability pathways are constrained. In our experiments, PEG-U, EHMA, and IDMA reduced the amount of monomer (i.e., UDMA) in the matrix, which then leads to a delayed vitrification point. Furthermore, high DVCs typically warrant the composites longevity [63] thus, reinforcing the use of high DVC UPE/IDMA and/or UPH/IDMA resins as polymer phase of multifunctional composites. Further, enforcement for such recommendation comes from the wettability study results. Contact angles of IDMA resins (63.2-65.5)⁰ coincide with the upper threshold reported for commercial resin-based composites (31.5-64.5)⁰[64]. High contact angle values imply lesser tooth staining, plaque accumulation, and pathogen adhesion/proliferation and, ultimately, lower the risk of secondary caries onset and progression [65].

The average FS of IDMA-containing resins ((70.5±3.2) MPa) is below the FS values reported for the composite resins ((87.8-126.5) MPa); [66]. It, however, matches the lower FS threshold values for micro-filled, mini-filled, polyacid-modified, and flowable composites ((66.6-147.2) MPa) [67]. The observed decrease in the FS could be attributed to the differences in the chain length of the constituent monomers in UPE control vs. IDMA-UPE formulations. IDMAs have significantly shorter chain lengths than PEG-U and/or UDMA. This decrease in chain continuity due to IDMAs addition to the matrix is likely to result in decreased resin continuity/imperfection and lead to a decrease in the material strength. On the other hand, higher DVCs attained in IDMA-UPE resins are most likely due to an overall increase in copolymer reactivity/monomer mobility due to IDMA incorporation. The preliminary kinetic data on polymerization of UPE and IDMA-UPE resins (study currently in progress) indicate that the rate of polymerization is significantly increased with IDMA incorporation vs. the UPE control support this explanation. Notwithstanding, the observed ~25% reduction in FS of IDMA containing copolymer vs. no-IDMA control should not disqualify IDMA/UPE resins from continued evaluation since they are primarily intended for use as Class V restoratives, where high strengths are not a primary requirement. Moreover, the unwanted effect on FS of copolymers could be amended by modifying the filler phase of the composites via introduction of reinforcing glass [66] in addition to the remineralizing ACP filler.

Although the full-scale mechanical evaluations are yet to be performed, it is highly encouraging that in milled ACP composites the attained solution Ca and P levels matched the ones detected in as-made ACP formulations (both being conducive to remineralization via apatite deposition). Using milled ACP with more homogeneous PSD is likely to yield composites with more uniform filler distribution within the polymer matrix, which should improve the composite's performance upon prolonged exposure to aqueous milieu. To achieve a desired balance between the AM capacity, mechanical stability and remineralization potential of multifunctional composites, tailoring the resin composition by adjusting the IDMAs levels, HEMA and/or EHMA may, eventually, be necessary. If AMRE composites underperform with respect to remineralization efficacy (i.e., less than 15%-20% enamel recovery [68, 69] and 30%-40% [70] dentin mineral

recovery), magnesium and/or iron-laced ACP, recently identified as the enduring amorphous phases in the mature mineralized tissues [71], will be employed as bioactive fillers.

Conclusion

IDMAs with enhanced purity were synthesized utilizing modified synthetic protocols. Their structures were confirmed by in-depth NMR and MS analysis. At accelerated leaching conditions, both IDMAs showed only minimal or no cellular toxicity. Incorporation of IDMAs improved the DVC of the resins, while not affecting resin's wettability. Incorporation of ACP filler yielded composites with pronounced remineralizing capacity. The observed reduction in FS should not prevent inclusion of IDMAs in the future design of Class V restoratives. The foreseen advantage of the proposed design is attaining AM protection via direct bacterial contact at the restoration interface rather than by the burst release of AM agent into oral milieu and reducing pathogens colonization, while having a minimal or no detrimental effect on mammalian cell viability. AMRE composite development is amenable to the National Institute of Dental and Craniofacial initiative focusing on novel Class V restoratives design (RFA-DE-16-007) and complementary to an earlier call for the improved resin composite materials that should outperform currently used Bis-GMA/TEGDMA materials (RFA-DE-13-001). Results of this study encourage further comprehensive evaluations of IDMAs as AM components of resins and/or composites.

Declaration of Conflicting Interests

The author(s) declared no potential conflicts of interest with respect to research, authorship, and/or publication of this article.

Disclaimer

Certain commercial materials and equipment are identified in this article for the sole purpose of adequately defining the experimental protocols. In no instance does such identification imply endorsement and/or recommendation by either the ADA Foundation or NIST, or that the material/equipment identified is the best available for the purpose.

Acronym list

ACP = amorphous calcium phosphate

Ag = silver

AM = antimicrobial

AMRE = antimicrobial and remineralizing

ANOVA = analysis of variance

bBrMbP = 2,2'-bis(bromomethyl)-1,1'-biphenyl

BEMA = 2-bromoethyl methacrylate

BHT = butylated hydroxytoluene

Bis-GMA = 2,2-bis[p-(2-hydroxy-3-methacryloxypropoxy)phenyl] propane

Ca = calcium

DMAEMA = 2-(N,N-dimethylamino)ethyl methacrylate

DMSO-d6 = deuterated dimethyl sulfoxide

DVC = degree of vinyl conversion

E = elastic modulus

4EDMAB = ethyl-4-N,N-dimethylamino benzoate

EHMA = ethyl 2-(hydroxymethyl)acrylate

FTIR = Fourier transform infrared spectroscopy

FS = flexural strength

HEMA = 2-hydroxyethyl methacrylate

HEPES = 4-(2-hydroxyethyl)piperazine-1-ethanesulfonic acid

HSQC = heteronuclear single quantum coherence

IDMA1 = 2-(methacryloyloxy)-N-(2-(methacryloyloxy)ethyl)-N,N-dimethylethan-1-aminium bromide

IDMA2 = N,N'-([1,1'-biphenyl]-2,2'-diylbis(methylene))bis(2-(methacryloyloxy)-N,N-dimethylethan-1-aminium) bromide

MDBP = methacryloyloxydodecylpyrimidinium bromide

MS = mass spectrometry

n = number of specimens (replicates; experimental runs)

NMR = nuclear magnetic resonance

P = phosphorus

PEG-U = poly(ethylene glycol) extended urethane dimethacrylate

PO4 = phosphate

PSD = particle size distribution

QA = quaternary ammonium

QA-MA = quaternary ammonium methacrylate

SEM = standard error of mean

SD = standard deviation

TEGDMA = triethylene glycol dimethacrylate

TMS = tetramethylsilane

UDMA = urethane dimethacrylate

UPE = UDMA/PEG-U/EHMA resin

UPH = UDMA/PEG-U/HEMA resin

XRD = X-ray diffraction

References

1. Imazato S. Antibacterial properties of resin composites and dentin bonding systems. Dent Mater. 2003; 19: 449-457.

2. Imazato S. Bio-active restorative materials with antibacterial effects: New dimension of innovation in restorative dentistry. Dent Mater J. 2009; 28: 11-19.

3. Cramer NB, JW Stansbury, CN Bowman. Recent advances and developments in composite dental restorative materials. J Dent Res. 2011; 90: 402-416.

4. Ferracane JL. Resin composite-state of the art. Dent Mater. 2011; 27: 29-38.

5. Cochrane NJ, Cai F, Huq NL, Burrow MF, Reynolds EC. New approaches to enhanced remineralization of tooth enamel. J. Dent. Res. 2010; 89: 1187-97.

6. Mickenautsch SG. Mount G, Yengopal V. Therapeutic effect of glass-ionomers: An overview of evidence. Aust Dental J. 2011; 56: 10-15.

7. Rodrigues JA, Lussi A, Seemann R, Neuhaus KW. Prevention of crown and root caries in adults. Periodontol 2000. 2011; 55: 231-249.

8. Skrtic D, Antonucci JM. Dental composites: Bioactive polymeric amorphous calcium phosphate-based, in Encyclopedia of Biomedical Polymers and Polymeric Biomaterials. 2015. CRC Press. 2443-2462.

9. Beniash E, Metzler RA, Lam RS, Gilbert PU. Transient amorphous calcium phosphate in forming enamel. J Struct Biol. 2009; 166: 133-143.

10. Bienek DR, Skrtic D. Utility of amorphous calcium phosphate-based scaffolds in dental/biomedical applications. Biointerface Res Appl Chem. 2017; 7: 1989-1994.

11. Dorozhkin SV. Amorphous calcium (ortho) phosphates. Acta Biomater. 2010; 6: 4457-4475.

12. Dorozhkin SV. Amorphous Calcium Orthophosphates: Nature, Chemistry and Biomedical Applications. Int J Mater Chem. 2012; 2: 19-46.

13. Zhao J, Liu Y, Sun WB, Yang X. First detection, characterization, and application of amorphous calcium phosphate in dentistry. J Dent Sci. 2012; 7: 316-323.

14. Pereira-Cenci T, Cenci MS, Fedorowicz Z, Marchesan MA. Antibacterial agents in composite restorations for the prevention of dental caries. Cochrane Database Syst Rev. 2009: Cd007819.

15. Jedrychowski JR, Caputo AA, Kerper S. Antibacterial and mechanical properties of restorative materials combined with chlorhexidines. J Oral Rehabil. 1983; 10: 373-381.

16. Osinaga PW, Grande RH, Ballester RY, Simionato MR, Delgado Rodrigues CR, Muench A. Zinc sulfate addition to glass-ionomer-based cements: influence on physical and antibacterial properties, zinc and fluoride release. Dent Mater. 2003; 19: 212-217.

17. Syafiuddin T, Hisamitsu H, Toko T, Igarashi T, Goto N, Fujishima A, et al. In vitro inhibition of caries around a resin composite restoration containing antibacterial filler. Biomaterials. 1997; 18: 1051-1057.

18. Takahashi Y, Imazato S, Kaneshiro AV, Ebisu S, Frencken JE, Tay FR. Antibacterial effects and physical properties of glass-ionomer cements containing chlorhexidine for the ART approach. Dent Mater. 2006; 22: 647-652.

19. Wiegand A, Buchalla W, Attin T. Attin, Review on fluoride-releasing restorative materials--fluoride release and uptake characteristics, antibacterial activity and influence on caries formation. Dent Mater. 2007; 23: 343-362.

20. Weng Y, Guo X, Chong VJ, Howard L, Richard L. Gregory et al., Synthesis and evaluation of a novel antibacterial dental resin composite with quaternary ammonium salts. J Biomed Sci Eng. 2011; 4: 147.

21. Cocco AR, Rosa WL, Silva AF, Lund RG, Piva E. A systematic review about antibacterial monomers used in dental adhesive systems: Current status and further prospects. Dent Mater. 2015; 31: 1345-1362.

22. Ebi N, Imazato S, Noiri Y, Ebisu S. Inhibitory effects of resin composite containing bactericide-immobilized filler on plaque accumulation. Dent Mater. 2001; 17: 485-491.

23. Imazato S, Tarumi H, Kato S, Ebisu S. Water sorption and colour stability of composites containing the antibacterial monomer MDPB. J Dent. 1999; 27: 279-283.

24. Thomé T, Mayer MP, Imazato S, Geraldo-Martins VR, Marques MM. In vitro analysis of inhibitory effects of the antibacterial monomer MDPB-containing restorations on the progression of secondary root caries. J Dent. 2009; 37: 705-711.

25. Antonucci JM. Polymerizable biomedical composition. Cite US patent No. 8,217,081 B2 2012: USA.

26. Imazato S, Imai T, Russell RR, Torii M, Ebisu S. Antibacterial activity of cured dental resin incorporating the antibacterial monomer MDPB and an adhesion-promoting monomer. J Biomed Mater Res. 1998; 39: 511-515.

27. Cheng L, Weir MD, Xu HH, Antonucci JM, Kraigsley AM, Lin NJ, et al. Antibacterial amorphous calcium phosphate nanocomposites with a quaternary ammonium dimethacrylate and silver nanoparticles. Dent Mater. 2012. 28: 561-572.

28. Cheng L, Zhang K, Zhou CC, Weir MD, Zhou XD, Xu HH. One-year water-ageing of calcium phosphate composite containing nano-silver and quaternary ammonium to inhibit biofilms. Int J Oral Sci. 2016; 8: 172-181.

29. Li F, Weir MD, Chen J, Xu HH. Comparison of quaternary ammonium-containing with nano-silver-containing adhesive in antibacterial properties and cytotoxicity. Dent Mater. 2013; 29: 450-461.

30. Melo MA, Cheng L, Weir MD, Hsia RC, Rodrigues LK, Xu HH. Novel dental adhesive containing antibacterial agents and calcium phosphate nanoparticles. J Biomed Mater Res B Appl Biomater. 2013; 101: 620-629.

31. Antonucci JM, Zeiger DN, Tang K, Lin-Gibson S, Fowler BO, Lin NJ. Synthesis and characterization of dimethacrylates containing quaternary ammonium functionalities for dental applications. Dent Mater. 2012; 28: 219-228.

32. Randolph LD, Palin WM, Bebelman S, Devaux J, Gallez B, Leloup G, et al. Ultra-fast light-curing resin composite with increased conversion and reduced monomer elution. Dent Mater. 2014; 30: 594-604.

33. American Society for Testing and Materials, Standard test method for agar diffusion cell culture screening for cytotoxicity. 2015, ASTM International: West Conshohocken, PA.

34. American Society for Testing and Materials, Standard practice for direct contact cell culture evaluation of materials for medical devices. 2015, ASTM International: West Conshohocken, PA.

35. Skrtic D, Antonucci JM. Bioactive polymeric composites for tooth mineral regeneration: Physicochemical and cellular aspects. J Funct Biomat. 2011; 2: 271-307.

36. Bienek DR, Frukhtbeyn SA, Giuseppetti AA, Okeke UC, Skrtic D. Antimicrobial monomers for polymeric dental restoratives: Cytotoxicity and physicochemical properties. J Funct Biomat. 2018; 9: 20.

37. Antonucci JM, Fowler BO, Weir MD, Skrtic D, Stansbury JW. Effect of ethyl-alpha-hydroxymethylacrylate on selected properties of copolymers and ACP resin composites. J Mater Sci Mater Med.

2008; 19: 3263-3271.

38. Snedecor G, Cochran W. Statistical Methods, 8th edition. 8th edn. 1989, Ames, IA: Iowa State University Press.

39. Neter J, Kutner MH, Nachtsheim CJ, Applied Linear Statistical Models. 4th edition ed. 1996, New York City, NY: McGraw-Hill Co.

40. Shapiro SS, Wilk WB. Analysis of variance test for normality (complete samples). Biometrika. 1965; 52: 591-611.

41. Dallas P, Sharma VK, Zboril R, Silver polymeric nanocomposites as advanced antimicrobial agents: classification, synthetic paths, applications, and perspectives. Adv Colloid Interface Sci. 2011; 166: 119-135.

42. Kawahara K, Tsuruda K, Morishita M, Uchida M. Antibacterial effect of silver-zeolite on oral bacteria under anaerobic conditions. Dent Mater. 2000; 16: 452-455.

43. Knetsch ML, LH Koole. New strategies in the development of antimicrobial coatings: the example of increasing usage of silver and silver nanoparticles. Polymers. 2011; 3: 340-366.

44. Yoshida KM, Tanagawa, Atsuta M. Characterization and inhibitory effect of antibacterial dental resin composites incorporating silver-supported materials. J Biomed Mater Res. 1999; 47: 516-522.

45. Imazato S, Ebi N, Takahashi Y, Kaneko T, Ebisu S, Russell RR. Antibacterial activity of bactericide-immobilized filler for resin-based restoratives. Biomaterials. 2003; 24: 3605-3609.

46. Beyth N, Yudovin-Farber I, Bahir R, Domb AJ, Weiss EI. Antibacterial activity of dental composites containing quaternary ammonium polyethylenimine nanoparticles against Streptococcus mutans. Biomaterials. 2006; 27: 3995-4002.

47. Cheng L, Zhang K, Weir MD, Melo MA, Zhou X, Xu HH. Nanotechnology strategies for antibacterial and remineralizing composites and adhesives to tackle dental caries. Nanomedicine. 2015; 10: 627-641.

48. Lee SB, Koepsel RR, Morley SW, Matyjaszewski K, Sun Y, Russell AJ. Permanent, nonleaching antibacterial surfaces. 1. Synthesis by atom transfer radical polymerization. Biomacromolecules. 2004; 5: 877-882.

49. Li F, Chai ZG, Sun MN, Wang F, Ma S, Zhang L, et al. Anti-biofilm effect of dental adhesive with cationic monomer. J Dent Res. 2009; 88: 372-376.

50. Li F, Chen J, Chai Z, Zhang L, Xiao Y, Fang M. Effects of a dental adhesive incorporating antibacterial monomer on the growth, adherence and membrane integrity of Streptococcus mutans. J Dent. 2009; 37: 289-296.

51. Ke Zhang, Lei Cheng, Michael D Weir, Yu-Xing Bai, Hockin HK Xu. Effects of quaternary ammonium chain length on the antibacterial and remineralizing effects of a calcium phosphate nanocomposite. Int J Oral Sci. 2016; 8: 45-53.

52. Zhang N, Melo MA, Chen C, Liu J, Weir MD, Bai Y, Xu HH. Development of a multifunctional adhesive system for prevention of root caries and secondary caries. Dent Mater. 2015; 31: 1119-1131.

53. Zhang N, Weir MD, Chen C, Melo MA, Bai Y, Xu HH. Orthodontic cement with protein-repellent and antibacterial properties and the release of calcium and phosphate ions. J Dent. 2016; 50: 51-59.

54. Inácio ÂS, Costa GN, Domingues NS, Santos MS, Moreno AJ, Vaz WL. Mitochondrial dysfunction is the focus of quaternary ammonium surfactant toxicity to mammalian epithelial cells. Antimicrob Agents Chemother. 2013; 57: 2631-2639.

55. Lichtenberg D, Opatowski E, Kozlov MM. Phase boundaries in mixtures of membrane-forming amphiphiles and micelle-forming amphiphiles. Biochim Biophys Acta. 2000; 1508: 1-19.

56. Preté PS, Domingues CC, Meirelles NC, Malheiros SV, Goñi FM, de Paula E, et al. Multiple stages of detergent-erythrocyte membrane interaction--a spin label study. Biochim Biophys Acta. 2011; 1808: 164-710.

57. Edmondson R, Broglie JJ, Adcock AF, Yang L. Three-dimensional cell culture systems and their applications in drug discovery and cell-based biosensors. Assay Drug Dev Technol. 2014; 12: 207-218.

58. Moharamzadeh K, Colley H, Murdoch C, Hearnden V, Chai WL, Brook IM. Tissue-engineered oral mucosa. J Dent Res, 2012; 91: 642-650.

59. Moharamzadeh K, Brook IM, Van Noort R, Scutt AM, Thornhill MH. Tissue-engineered oral mucosa: a review of the scientific literature. J Dent Res. 2007; 86: 115-124.

60. Padova DM. Oral Mucosa-on-a-Chip for Cytotoxicity Testing of Biomaterials on Human Gingival Cells. in Biomedical Engineering Society 2016 Annual Meeting. 2016. Minneapolis MN.

61. Antonucci JM, Skrtic D. Bioactive and biocompatible polymeric composites based on amorphous calcium phosphate, in Integrated Biomaterials for Medical Applications, M. Ramalingam, et al., Editors. 2012, Scrivener Publishing: Salem. 67-119.

62. Skrtic D, Antonucci JM. Dental composites based on amorphous calcium phosphate - resin composition/physicochemical properties study. J Biomater Appl. 2007; 21: 375-393.

63. Braga RR, Ferracane JL. Contraction stress related to degree of conversion and reaction kinetics. J Dent Res. 2002; 81: 114-118.

64. da Silva EM, Almeida GS, Poskus LT, Guimarães JG. Relationship between the degree of conversion, solubility and salivary sorption of a hybrid and a nanofilled resin composite. J Appl Oral Sci. 2008; 16: 161-166.

65. Fu J, Liu W, Hao Z, Wu X, Yin J, Panjiyar A, et al. Characterization of a low shrinkage dental composite containing bismethylene spiroorthocarbonate expanding monomer. Int J Mol Sci. 2014; 15: 2400-2412.

66. Della Bona A, Benetti P, Borba M, Cecchetti D. Flexural and diametral tensile strength of composite resins. Braz Oral Res. 2008; 22: 84-89.

67. Chung SM, Yap AU, Chandra SP, Lim CT. Flexural strength of dental composite restoratives: comparison of biaxial and three-point bending test. J Biomed Mater Res B Appl Biomater. 2004; 71: 278-283.

68. Langhorst SE, O'Donnell JN, Skrtic D. In vitro remineralization of enamel by polymeric amorphous calcium phosphate composite: Quantitative microradiographic study. Dent Mater. 2009; 25: 884-891.

69. Skrtic D, Hailer AW, Takagi S, Antonucci JM, Eanes ED. Quantitative assessment of the efficacy of amorphous calcium phosphate/methacrylate composites in remineralizing caries-like lesions artificially produced in bovine enamel. J Dent Res. 1996; 75: 1679-1686.

70. Dickens SH, Flaim GM, Takagi S. Mechanical properties and biochemical activity of remineralizing resin-based Ca-PO4 cements. Dent Mater. 2003; 19: 558-566.

71. Gordon LM, Cohen MJ, MacRenaris KW, Pasteris JD, Seda T, Joester D. Dental materials. Amorphous intergranular phases control the properties of rodent tooth enamel. Science. 2015; 347: 746-750.

72. Bienek DR. Physiochemical characterization and biocompatibility of ionic dimethacrylates for dental restorations. Trans Soc Biomater. (in press) 2018.